Beyond 5G Localization via Sidelinks in Industrial IoT scenarios

Gianluca Torsoli*, Moe Z. Win†, and Andrea Conti*

*Department of Engineering and CNIT, University of Ferrara, Via Saragat 1, 44122 Ferrara, Italy
(e-mail: gianluca.torsoli@unife.it, a.conti@ieee.org)
†Laboratory for Information and Decision Systems, Massachusetts Institute of Technology, Cambridge, MA 02139 USA
(e-mail: moewin@mit.edu)

***Abstract*—Location awareness is a fundamental enabler for several emerging fifth generation (5G) and beyond wireless applications. In particular, since Release 18 the 3rd Generation Partnership Project (3GPP) is putting an effort on the standardization of sidelink (SL) localization. This can be particularly important both to enhance the localization capabilities of the 5G network and to provide location awareness in partial-coverage conditions. However, SL localization poses additional challenges with respect to conventional downlink and uplink localization, such as the uncertainty in the position of the SL nodes. This paper proposes two algorithms based on soft information (SI) for SL localization in 5G and beyond wireless networks. Results for 3GPP settings in an indoor factory scenario demonstrate the effectiveness of the proposed approaches to improve the localization accuracy in full-coverage conditions, as well as to provide location awareness in partial-coverage conditions.**

***Index Terms*—5G, sidelink, localization, device-to-device, 3GPP, wireless networks**

I. Introduction

Localization via device-to-device links, [1], [2], also referred to as sidelinks (SLs) in the 3rd Generation Partnership Project (3GPP) technical specifications, is expected to be a key enabler for several applications in fifth generation (5G) and beyond wireless networks [3], including autonomous vehicles [4], Internet-of-Things (IoT) [5], Industrial Internet-of-Things (IIoT) [6], vehicle-to-everything (V2X) [7], and public safety [8]. With Release 18, the 3GPP is putting increasing effort into the standardization of SLs both for communication and localization. In this context, the 3GPP defines three possible conditions for localization employing SLs (herafeter referred to as SL localization), namely full-coverage (FC), partial-coverage (PC), the out-of-coverage (OC) conditions [9]. An example of 5G network where all the aforementioned conditions are present is depicted in Fig. 1. In particular, SL localization, enables improving the localization accuracy in the FC conditions, extending the localization coverage in the PC conditions, and providing relative localization in the OC conditions. However, achieving the performance required by 3GPP for SL localization is particularly challenging [9]–[11]. Wireless environments often are characterized by harsh multipath propagation and frequent non-line-of-sight (NLOS) conditions, which typically degrade the localization accuracy

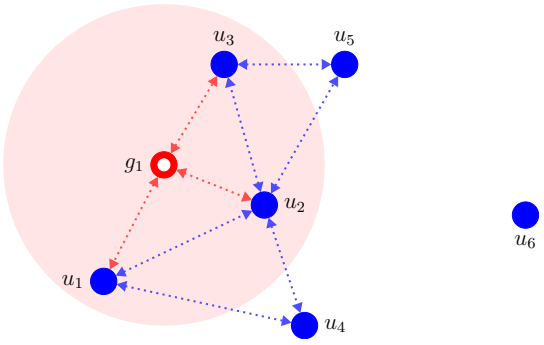

Fig. 1. Example of SL localization: the gNBs g_1 communicates with the UEs u_1, u_2, and u_3 which are in FC and can cooperate to enhance their location awareness. The UEs u_4 and u_5 are in PC and require exchanging information with the other UEs to be localized. Finally, the UE u_6 is in an OC condition since it cannot communicate with any gNB or UE.

[12]. Moreover, SL localization poses additional challenges with respect to localization via downlink (DL) and uplink (UL) with gNBs. These include the uncertainty in the position of the SL network nodes, the difficulty in obtaining precise synchronization among the UEs [13], and the coexistence between SL communication and localization [14], [15].

3GPP documents [16] show extensive performance for SL localization that are typically obtained using conventional localization algorithms, also referred to as single-value estimate (SVE)-based algorithms [17]. However, these approaches are not able to satisfy the localization service level requirements in complex wireless environments [1].

The goal of this paper is to demonstrate the capabilities of SL localization to provide accurate localization in 5G and beyond wireless networks. The key idea is to leverage the recently proposed soft information (SI)-based localization. Such approach exploits machine learning techniques to provide a probabilistic description of the relationship between UE position, measurements, contextual information [18], [19].

This paper presents a SI-based approach for SL localization in beyond 5G wireless networks. The key contributions of this paper can be summarized as follows:

979-8-3503-0405-3/24/$31.00 ©2024 IEEE

- development of SI-based iterative algorithms to improve the localization accuracy in the FC conditions and to extend the localization coverage in the PC conditions via SLs measurements; and
- quantification of the performance provided by the proposed algorithms in a 3GPP-standardized factory scenario.

The remainder of the paper is organized as follows. Section II briefly describes SL localization in 5G and beyond networks; Section III presents two case studies in the 3GPP-standardized indoor factory (InF)-SH scenario; finally, Section IV provides our conclusions.

Notations: A random variable and its realization are denoted by x and x; a random vector and its realization are denoted by $\mathbf{x}$ and $\boldsymbol{x}$; a set is denoted by calligraphic fonts as $\mathcal{X}$. For a vector $\boldsymbol{x}$, its transpose is denoted by $\boldsymbol{x}^{\mathrm{T}}$. The function $f_{\mathbf{x}}(\boldsymbol{x};\boldsymbol{\theta})$ indicates the probability density function (PDF) of a continous random vector $\mathbf{x}$ parametrized by $\boldsymbol{\theta}$.

II. Localization in 5G networks

Consider a network composed of N_{b} gNBs indexed by $j \in \mathcal{N}_{\mathrm{b}} = \{1, 2, \ldots, N_{\mathrm{b}}\}$ with known positions and N_{u} UEs indexed by $i \in \mathcal{N}_{\mathrm{u}} = \{1, 2, \ldots, N_{\mathrm{u}}\}$ with unknown positions. Denoting by $\mathring{\mathcal{N}}_{\mathrm{u}}$ and $\breve{\mathcal{N}}_{\mathrm{u}}$ the index set of UEs in FC and PC, respectively, then $\mathcal{N}_{\mathrm{u}} = \mathring{\mathcal{N}}_{\mathrm{u}} \cup \breve{\mathcal{N}}_{\mathrm{u}}$.

A localization algorithm aims to estimate the positions of the i-th UE leveraging a collection of measurements $\{\boldsymbol{y}_{i,j'}\}_{j' \in \mathcal{N}^{(i)}}$ obtained exchanging information with the gNBs via DL and/or UL and with the other UEs via SL. The index set $\mathcal{N}^{(i)} = \mathcal{N}_{\mathrm{b}}^{(i)} \cup \mathcal{N}_{\mathrm{u}}^{(i)}$ denotes the complete index set of the nodes to which the i-th UE can exchange information, where $\mathcal{N}_{\mathrm{b}}^{(i)} \subseteq \mathcal{N}_{\mathrm{b}}$, and $\mathcal{N}_{\mathrm{u}}^{(i)} \subseteq \mathcal{N}_{\mathrm{u}} \setminus \{i\}$ (considering only inter-node measurements and no intra-node measurements). Measurements may include time-, angle-, or power-based metrics, waveform samples, and any combination of them. Each measurement $\boldsymbol{y}_{i,j'}$ is related to a positional feature vector $\boldsymbol{\theta}(\boldsymbol{p}_i, \boldsymbol{p}_{j'})$ which is a function of the position of both the i-th UE and the j'-th element of $\mathcal{N}^{(i)}$. Assuming only time-based measurements, a UE can be defined in FC for localization if it can communicate with at least 3 gNBs, and in PC if it can communicate only with other UEs, and at least 3 of them are in FC.

In 3GPP specifications for 5G localization, measurements are obtained transmitting and processing tailored reference signals (RSs) for localization. In particular, localization in DL is performed via the DL-positioning reference signal (PRS) while localization in UL is performed via the UL-sounding reference signal (SRS) [20]. The standardization of the signal structure for SL localization is still under discussion by the 3GPP [16].

A. SL-PRS physical structure

Currently, the 3GPP technical specifications consider for the design of the SL-PRS the reuse of the orthogonal frequency division multiplexing (OFDM)-based DL-PRS signal structure. The OFDM structure of the DL-PRS is described in detail in [21] and is divided into frames, subframes, and slots in the time domain and into resource blocks in the frequency domain. According to the 3GPP nomenclature, a resource element (RE), indexed by (k, l), denotes the k-th subcarrier of the l-th symbol in the OFDM time-frequency grid. The PRS is obtained by allocating to the REs symbols obtained by modulating via quadrature phase-shift keying (QPSK) a 31-bit long Gold sequence, initialized based on the physical cell identity (PCI) [21]. In the frequency domain, the PRS structure is arranged in a comb structure, where symbols are allocated only in one out of K subcarriers. For SL-PRS, potential candidate values for the comb size are $K \in \{1, 2, 4, 6, 8, 12\}$. In the time domain, L consecutive symbols within a slot are used [16]. According to 3GPP specifications for SL localization, a fully-staggered configuration (i.e., $L = K$), and a partially staggered configuration (i.e., $L < K$) are considered. Then, the discrete OFDM signal for the l-th symbol is given by

$$s_l[n] = \frac{1}{\sqrt{N_{\mathrm{F}}}} \sum_{k=0}^{N_{\mathrm{F}}} a_{k,l} \exp\left\{\frac{2\pi n k}{N_{\mathrm{F}}}\right\} \tag{1}$$

where $a_{k,l}$ is the symbol to be allocated in the (k, l) RE, and $N_{\mathrm{F}} = N_{\mathrm{SC}}\, N_{\mathrm{RB}}$, in which $N_{\mathrm{SC}} = 12$ and N_{RB} is the number of resource blocks allocated [21].

B. 5G measurements for localization

The RSs can be transmitted both in frequency range 1 (FR1) (i.e., carrier frequency below 7.125 GHz), and in frequency range 2 (FR2) at millimeter waves (i.e., carrier frequency between 24.25 GHz and 52.6 GHz). By processing the received SL-PRS, several measurements can be extracted to infer the UEs position. According to 3GPP standardization, the time measurements considered for SL localization are the SL-round-trip time (RTT) (obtained via the two-way transmission of the SL-PRS), and the SL-time difference-of-arrival (TDOA) (obtained by subtracting the SL-time-of-arrival (TOA) of a reference UE to the SL-TOA estimated with respect to the other UEs) [16], [19].

Note that SL-RTT is a preferred choice over SL-TDOA for SL localization for two main reasons. First, it does not require accurate synchronization between the SL nodes (i.e., the UEs serving as anchors for localization). Second, it removes the problem of selecting the reference base station [22].

Similarly, the DL-PRS and the UL-SRS can be processed to obtain measurements for localization, such as the DL-TDOA, the UL-TDOA, and the RTT [23], [24]

C. SI for SL localization

SI-based localization has been recently proposed to enhance the localization capabilities of wireless networks and has already been proven to be effective in the 5G and beyond ecosystems [19]. In particular, SI-based localization is based on a machine learning-based probabilistic framework which

Algorithm 1 Localization in FC with SL measurements

1. Estimate the position of all the UEs in FC using measurements obtained exchanging RSs with the gNBs
   1: **for** $i \in \mathring{\mathcal{N}}_{\mathrm{u}}$ **do**

$$\check{\boldsymbol{p}}_i = \arg\max_{\tilde{\boldsymbol{p}}} \prod_{j \in \mathcal{N}_{\mathrm{b}}^{(i)}} \mathcal{L}_{\boldsymbol{y}_{i,j}}(\boldsymbol{\theta}(\tilde{\boldsymbol{p}}, \boldsymbol{p}_j))$$

   2: **end for**
2. Refine the position estimation of the UEs in FC leveraging the information obtained from SL measurements
   1: **for** $i \in \mathring{\mathcal{N}}_{\mathrm{u}}$ **do**

$$\hat{\boldsymbol{p}}_i = \arg\max_{\tilde{\boldsymbol{p}}} \prod_{j \in \mathcal{N}_{\mathrm{b}}^{(i)}} \mathcal{L}_{\boldsymbol{y}_{i,j}}(\boldsymbol{\theta}(\tilde{\boldsymbol{p}}, \boldsymbol{p}_j)) \times \prod_{i' \in \mathring{\mathcal{N}}_{\mathrm{u}}^{(i)}} \mathcal{L}_{\boldsymbol{y}_{i,i'}}(\boldsymbol{\theta}(\tilde{\boldsymbol{p}}, \check{\boldsymbol{p}}_{i'}))$$

   2: **end for**

enables to overcome the limitations of conventional localization algorithms [12], [18]. Specifically, the probabilistic information related to the measurements, also referred to as soft feature information (SFI), is given by

$$\mathcal{L}_{\boldsymbol{y}_{i,j}}(\boldsymbol{\theta}_{i,j}) \propto f_{\mathbf{y}}(\boldsymbol{y}_{i,j}; \boldsymbol{\theta}(\boldsymbol{p}_i, \boldsymbol{p}_j)) \tag{2a}$$

$$\mathcal{L}_{\boldsymbol{y}_{i,i'}}(\boldsymbol{\theta}_{i,i'}) \propto f_{\mathbf{y}|\mathbf{p}}(\boldsymbol{y}_{i,i'} | \boldsymbol{\theta}(\boldsymbol{p}_i, \mathbf{p}_{i'})) \tag{2b}$$

where (2a) and (2b) refer to the SFI related to measurements obtained by the i-th UE exchanging information with the j-th gNB and with the i'-th UE, respectively. In complex wireless environments, the SFI is obtained as proportional to a generative model, (i.e., an approximation of the joint probability distribution of measurements and positional features) which can be obtained via a density estimation process. Let $\boldsymbol{x} = [\boldsymbol{y}, \boldsymbol{\theta}]^{\mathrm{T}}$ and let $\boldsymbol{z} = \mathcal{S}(\boldsymbol{x})$ where $\mathcal{S}(\cdot)$ denotes a sphering transformation [25]. Then, an effective approach for fitting the generative model is via a Gaussian mixture model (GMM) with N_{M} components, which is given by

$$f(\boldsymbol{z}; \{\alpha_k, \boldsymbol{\mu}_k, \boldsymbol{\Sigma}_k\}_{k=1}^{N_{\mathrm{M}}}) = \sum_{k=1}^{N_{\mathrm{M}}} \alpha_k \varphi(\boldsymbol{z}; \boldsymbol{\mu}_k, \boldsymbol{\Sigma}_k) \tag{3}$$

where α_k, $\boldsymbol{\mu}_k$, and $\boldsymbol{\Sigma}_k$ denote the weight, the mean, and the covariance of the k-th component of the GMM. The parameters of the GMM can be fit via a data-driven approach using the expectation-maximization algorithm [26].

Given a set of measurements $\{\boldsymbol{y}_{i,j'}\}_{j' \in \mathcal{N}^{(i)}}$, the position of the i-th UE can be inferred via maximum likelihood estimation after the evaluation of (3) [18]. While SI-based localization using only UL or DL measurements has been already studied extensively [12], [19], we propose two algorithms to leverage also the information provided by SL measurements.

Algorithm 1 describes an approach based on SI for improving localization accuracy leveraging the SL measurements in the FC condition. Specifically, in the first step the UEs are localized via DL or UL measurements. Then, the information exchanged between the UEs via SL, together with the positions estimated in the previous step, is used to improve the position estimation of all the UEs in FC.

Algorithm 2 Localization in PC with SL measurements

1. Estimate the position $\{\hat{\boldsymbol{p}}_i\}_{i \in \mathring{\mathcal{N}}_{\mathrm{u}}}$ of all the UEs in FC via Algorithm 1.
2. Estimate the position of UEs in PC leveraging only the information from SL measurements
   1: **for** $i \in \check{\mathcal{N}}_{\mathrm{u}}$ **do**

$$\hat{\boldsymbol{p}}_i = \arg\max_{\tilde{\boldsymbol{p}}} \prod_{i' \in \mathring{\mathcal{N}}_{\mathrm{u}}^{(i)}} \mathcal{L}_{\boldsymbol{y}_{i,i'}}(\boldsymbol{\theta}(\tilde{\boldsymbol{p}}, \hat{\boldsymbol{p}}_{i'}))$$

   2: **end for**

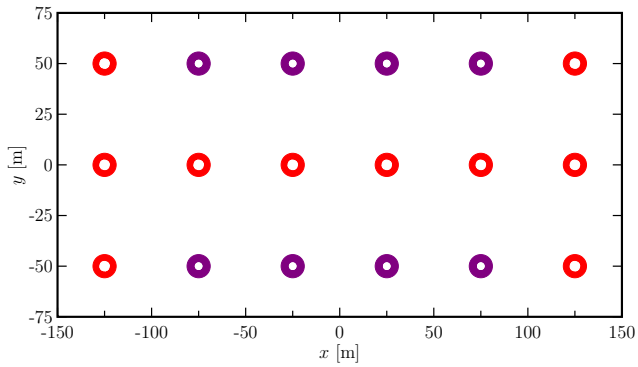

Fig. 2. Layout of the 3GPP standardized InF-SH scenario, the annuluses indicate the gNB positions. In the results, Case I considers all the 18 gNBs in the scenario, while Case II considers only 8 gNBs (i.e., the violet gNBs in the figure).

Algorithm 2 describes an approach based on SI for providing location awareness to UEs in PC via SL measurements. Specifically, in the first step Algorithm 1 is used to localize the UEs in FC in the network. Then, the information exchanged between the UEs via SL, together with the positions estimated in the previous step, is used to infer the position of all the UEs in PC. Hence, such approach enables the localization of UEs in PC using as prior knowledge only the gNBs positions.

III. Case Studies

In this section, results are reported for localization with SL measurements in 3GPP scenarios. In particular, the effectiveness of the algorithms proposed in the previous section is shown. Results are validated in the 3GPP-compliant InF-SH scenario, whose layout is reported in Fig. 2. Such scenario describes a wide industrial factory area with a low obstacle density [27]. Two case studies are evaluated in this scenario, namely Case I, that considers 18 gNBs, and Case II, that considers only 8 gNBs of the original layout. The DL-PRS and the UL-SRS are transmitted with a bandwidth of 100 MHz and a central frequency of 3.5 GHz in FR1. The SL-PRS is created

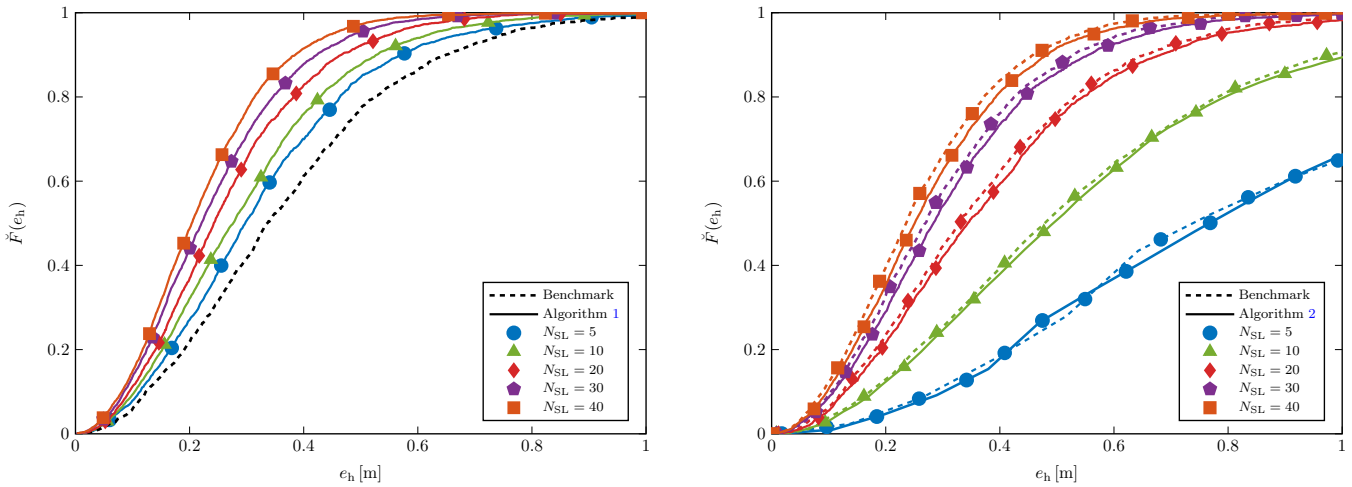

Fig. 3. Localization performance for the Case I of the InF-SH scenario. The performance are reported in terms of ECDF of the horizontal localization error varying the number of SL nodes for the (a) Algorithm 1 in the FC scenario; and (b) Algorithm 2 in the PC condition.

TABLE I
RELEVANT LOCALIZATION ERROR PERCENTILES FOR CASE I [m]

	N_SL	Configuration	50th	67th	80th	90th
FC	–	Benchmark	0.33	0.43	0.53	0.65
	5	Algorithm 1	0.30	0.38	0.46	0.57
	10	Algorithm 1	0.28	0.35	0.43	0.53
	20	Algorithm 1	0.24	0.30	0.38	0.46
	30	Algorithm 1	0.22	0.28	0.34	0.42
	40	Algorithm 1	0.20	0.25	0.31	0.38
PC	5	Benchmark	0.80	1.10	1.37	2.28
		Algorithm 2	0.80	1.14	1.65	3.16
	10	Benchmark	0.49	0.64	0.79	0.99
		Algorithm 2	0.51	0.65	0.80	1.04
	20	Benchmark	0.33	0.43	0.53	0.65
		Algorithm 2	0.34	0.46	0.55	0.68
	30	Benchmark	0.26	0.35	0.43	0.53
		Algorithm 2	0.28	0.36	0.44	0.55
	40	Benchmark	0.23	0.30	0.37	0.46
		Algorithm 2	0.25	0.32	0.39	0.48

according to Sec. II-A, and it is transmitted using $K = L = 4$ with a bandwidth of 100 MHz and a central frequency of 6 GHz. The DL-PRS and the UL-SRS are processed to estimate the RTT of the UEs in FC. Similarly, via the transmission of the SL-PRS between the UEs, it is possible to estimate the SL-RTT. The RTT and SL-RTT are the only measurements used by Algorithm 1 and Algorithm 2 to localize the UEs. The results are obtained in full compliance with 3GPP technical reports. Specifically, the RS are generated according to the specifications in [21]. All the parameters of the UEs and of the gNBs, including antenna patterns, transmitted power, and noise figure are set for the InF-SH scenario according to [27], [28]. The wireless channels are generated with spatial consistency according to [27] using the QuaDRiGa channel simulator [29].

To evaluate the performance, 100 random instantiations of the InF-SH scenario are generated, and for each of them, $N_\mathrm{SL} + 1$ UEs, with $N_\mathrm{SL} = 5, 10, 20, 30$ and 40, are deployed with random positions and orientations. We assume that each UE can communicate with N_SL UEs via SL and with all or none the gNBs if in FC or in PC, respectively. A 10-fold cross-validation technique [26] is used to compute the ECDF $\breve{F}(e_\mathrm{h})$ of the horizontal localization error e_h for the different configurations.

To showcase the effectiveness of the proposed algorithms, different benchmarks are considered. Specifically, to evaluate the performance of Algorithm 1, we consider as benchmark SI-based localization using only RTT measurements, demonstrating the effectiveness of the proposed approach in fusing the information obtained via SL measurements to improve the localization accuracy. Differently, for Algorithm 2, we consider as benchmark SI-based localization using only SL-RTT measurements, assuming that the positions of the SL nodes are known a priori. This enables demonstrating the effectiveness of the proposed approach to localize UEs in PC, as well as to showcase the resilience of Algorithm 2 to the uncertainty on the position of the SL nodes.

A. Results for Case I

Fig. 3a shows the performance in Case I of Algorithm 1 in terms of the ECDFs of the horizontal localization error. It can be observed that for all the configurations considered the use of SL measurements is able to improve the localization performance. In particular, Algorithm 1 provides a performance gain at the 90th percentile, with respect to the

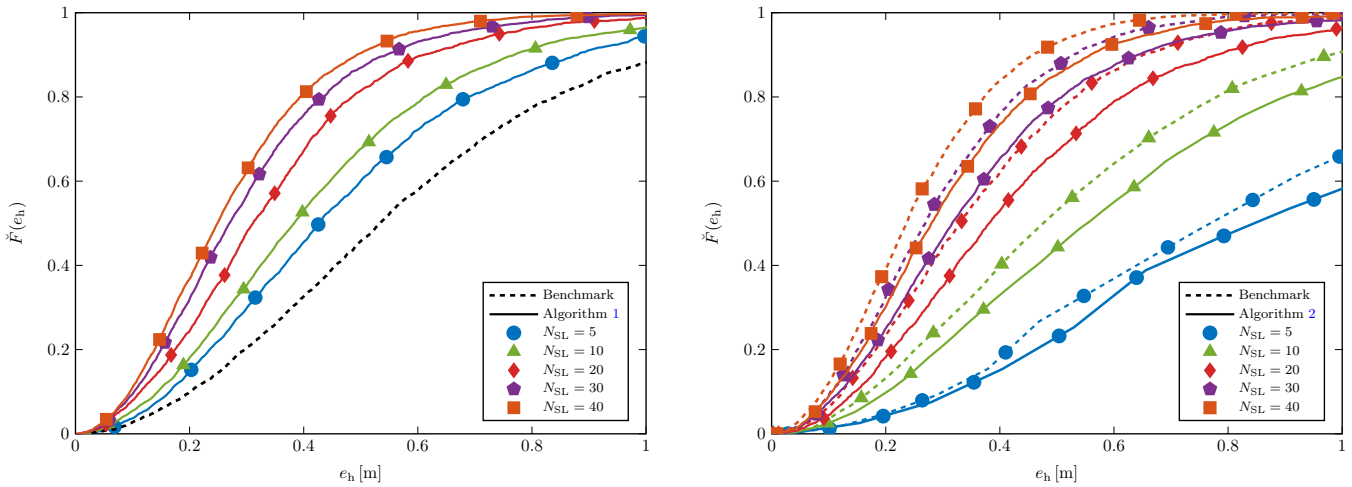

Fig. 4. Localization performance for the Case II of the InF-SH scenario. The performance are reported in terms of ECDF of the horizontal localization error varying the number of SL nodes for the (a) Algorithm 1 in the FC condition; and (b) Algorithm 2 in the PC condition.

benchmark, equal to 12%, 18%, 29%, 35%, and 41% for the cases with $N_{SL} = 5$, 10, 20, 30, and 40, respectively. Note that while the benchmark (i.e., SI-based localization using only RTT measurements) already provides sub-meter localization accuracy at the 90th percentile, the use of the SI obtained via SL allows to obtain a localization error below 0.5 m at the 90th percentile if $N_{SL} \geqslant 20$.

Fig. 3b shows the performance in Case I of Algorithm 2 in terms of the ECDFs of the horizontal localization error. It can be observed that for every number of SL nodes considered, Algorithm 2 approaches the benchmark, with a distance of a few centimeters at every percentile. In particular, it can be observed that for all the configurations considered, Algorithm 2 enables localizing the UEs in PC with a sub-meter localization accuracy at the 90th percentile. For example, considering $N_{SL} = 20$, it can be observed that the localization accuracy is around 45 cm at the 67th percentile, around 55 cm at the 80th percentile, around 70 cm at the 90th percentile, and around 1 m at the 99th percentile. Further details on the localization performance provided by Algorithm 1 and Algorithm 2 in Case I are reported in Table I.

TABLE II
RELEVANT LOCALIZATION ERROR PERCENTILES FOR CASE II [m]

	N_{SL}	Configuration	50th	67th	80th	90th
FC	–	Benchmark	0.53	0.69	0.84	1.03
	5	Algorithm 1	0.42	0.56	0.69	0.88
	10	Algorithm 1	0.38	0.50	0.61	0.77
	20	Algorithm 1	0.31	0.40	0.48	0.60
	30	Algorithm 1	0.27	0.35	0.43	0.55
	40	Algorithm 1	0.25	0.32	0.39	0.49
PC	5	Benchmark	0.83	1.10	1.37	2.28
		Algorithm 2	0.90	1.28	1.78	3.67
	10	Benchmark	0.49	0.64	0.79	0.99
		Algorithm 2	0.56	0.73	0.90	1.16
	20	Benchmark	0.33	0.43	0.53	0.65
		Algorithm 2	0.38	0.49	0.61	0.78
	30	Benchmark	0.26	0.35	0.43	0.53
		Algorithm 2	0.31	0.42	0.51	0.64
	40	Benchmark	0.23	0.30	0.37	0.46
		Algorithm 2	0.28	0.36	0.45	0.56

B. Results for Case II

Fig. 4a shows the performance in Case II of Algorithm 1 in terms of the ECDFs of the horizontal localization error. It can be observed that for all the configurations considered the use of SL measurements is able to improve the localization performance. In particular, Algorithm 1 provides a performance gain at the 90th percentile with respect to the benchmark equal to 14%, 25%, 40%, 46%, and 52% for the cases with $N_{SL} = 5$, 10, 20, 30, and 40, respectively. Note that while the benchmark (i.e., SI-based localization using only RTT measurements) provides approximately 1m̀ localization accuracy at the 90th percentile, the use of the SI obtained via SL allows to obtain a localization error below 0.9 m at the 90th percentile if $N_{SL} \geqslant 5$.

Fig. 4b shows the performance in Case II of Algorithm 2 in terms of the ECDFs of the horizontal localization error. It can be observed that for every number of SL nodes considered, Algorithm 2 approaches the benchmark, with a distance of some centimeters at every percentile. In particular, it can be observed that Algorithm 2 enables localizing the UEs in PC with a sub-meter localization accuracy at the 90th percentile if $N_{SL} \geqslant 20$. For example, considering $N_{SL} = 20$, it can be observed that the localization accuracy is around 50 cm

at the 67th percentile, around 60 cm at the 80th percentile, and around 80 cm at the 90th percentile. Further details on the localization performance provided by Algorithm 1 and Algorithm 2 in Case II are reported in Table II.

IV. Final Remark

This paper presented two soft information (SI)-based algorithms for sidelink (SL) localization in fifth generation (5G) and beyond wireless networks. We demonstrated that SL measurements can improve the estimation of the user equipments (UEs) positions in the full-coverage (FC) conditions, as well as extend the localization coverage to the UEs in the partial-coverage (PC) conditions. Results in a 3rd Generation Partnership Project (3GPP) industrial factory scenario demonstrate the effectiveness of the proposed algorithms, and showcase how leveraging SL measurements is fundamental to enhance the localization capabilities of 5G networks. The proposed algorithms represent a step towards achieving fully cooperative localization via SLs in 5G and beyond wireless networks.

Acknowledgment

The fundamental research described in this paper was supported, in part, by the Office of Naval Research under Grant N62909-22-1-2009, by the National Science Foundation under Grant CNS-2148251, and by funds from federal agency and industry partners in the RINGS program.

References

[1] *Technical Specification Group Radio Access Network; Technical Specification Group Services and System Aspects; Study on positioning use cases*, 3GPP™ Std. TR 22.872 V16.1.0, Sept. 2018, Release 16.

[2] A. Conti *et al.*, "Location awareness in beyond 5G networks," *IEEE Commun. Mag.*, vol. 59, no. 11, pp. 22–27, Nov. 2021, special issue on *Location Awareness for 5G and Beyond*.

[3] K. Ganesan, "5G advanced: Sidelink evolution," *IEEE Commun. Stand. Mag.*, vol. 7, no. 1, pp. 58–63, 2023.

[4] C. Diaz-Vilor, A. Lozano, and H. Jafarkhani, "Cell-free UAV networks: Asymptotic analysis and deployment optimization," *IEEE Trans. Wireless Commun.*, vol. 22, no. 5, pp. 3055–3070, 2023.

[5] A. Elzanaty, A. Guerra, F. Guidi, D. Dardari, and M.-S. Alouini, "Toward 6G holographic localization: Enabling technologies and perspectives," *IEEE Internet Things Mag.*, vol. 6, no. 3, pp. 138–143, 2023.

[6] Y. Lu, M. Koivisto, J. Talvitie, E. Rastorgueva-Foi, M. Valkama, and E. Simona Lohan, "Cooperative positioning system for industrial IoT via mmWave device-to-device communications," in *IEEE Semiannual Vehicular Technology Conference*, Helsinki, Finland, 2021, pp. 1–7.

[7] N. Decarli, A. Guerra, C. Giovannetti, F. Guidi, and B. M. Masini, "V2X sidelink localization of connected automated vehicles," *IEEE J. Sel. Areas Commun.*, vol. 42, no. 1, pp. 120–133, 2024.

[8] N. Chukhno, A. Orsino, J. Torsner, A. Iera, and G. Araniti, "5G NR sidelink multi-hop transmission in public safety and factory automation scenarios," *IEEE Netw.*, pp. 1–7, 2023.

[9] *Technical Specification Group Radio Access Network: Study on scenarios and requirements of in-coverage, partial coverage, and out-of-coverage NR positioning use cases*, 3rd Generation Partnership Project 3GPP™ TR 38.845 V17.0.0, Sep. 2021, Release 17.

[10] *Technical Specification Group Services and System Aspects; Service requirements for the 5G system; Stage 1*, 3GPP™ Std. TS 22.261 V19.1.0, Dec. 2022, Release 19.

[11] 5GAA, "System architecture and solution development; high accuracy positioning for C-V2X," www.5gaa.org, Feb. 2021.

[12] G. Torsoli, M. Z. Win, and A. Conti, "Blockage intelligence in complex environments for beyond 5G localization," *IEEE J. Sel. Areas Commun.*, vol. 41, no. 6, pp. 1688–1701, Jun. 2023, special issue on *3GPP Technologies: 5G-Advanced and Beyond*.

[13] S.-W. Ko, H. Chae, K. Han, S. Lee, D.-W. Seo, and K. Huang, "V2X-based vehicular positioning: Opportunities, challenges, and future directions," *IEEE Wireless Commun.*, vol. 28, no. 2, pp. 144–151, 2021.

[14] N. Decarli, S. Bartoletti, A. Bazzi, R. A. Stirling-Gallacher, and B. M. Masini, "Performance characterization of joint communication and sensing with beyond 5G NR-V2X sidelink," *IEEE Trans. Veh. Technol.*, pp. 1–16, 2024, *early access*.

[15] G. Kwon, A. Conti, H. Park, and M. Z. Win, "Joint communication and localization in millimeter wave networks," *IEEE J. Sel. Topics Signal Process.*, vol. 15, no. 6, pp. 1439–1454, Nov. 2021, special issue on *Joint Communication and Radar Sensing for Emerging Applications*.

[16] *Technical Specification Group Radio Access Network; Study on expanded and improved NR positioning*, 3GPP™ Std. TR 38.859 V18.0.0, Jan. 2023, Release 18.

[17] C. Mensing and S. Plass, "Positioning algorithms for cellular networks using TDOA," in *Proc. IEEE Int. Conf. Acoustics, Speech, and Signal Process.*, vol. 4, 2006, pp. IV–IV.

[18] A. Conti, S. Mazuelas, S. Bartoletti, W. C. Lindsey, and M. Z. Win, "Soft information for localization-of-things," *Proc. IEEE*, vol. 107, no. 11, pp. 2240–2264, Nov. 2019.

[19] F. Morselli, S. M. Razavi, M. Z. Win, and A. Conti, "Soft information based localization for 5G networks and beyond," *IEEE Trans. Wireless Commun.*, vol. 22, no. 12, pp. 9923–9938, Dec. 2023.

[20] *Technical Specification Group Radio Access Network; NG Radio Access Network (NG-RAN); Stage 2 functional specification of User Equipment (UE) positioning in NG-RAN*, 3GPP™ Std. TS 38.305 V17.3.0, Jan. 2023, Release 17.

[21] *Technical Specification Group Radio Access Network; NR; Physical channels and modulation*, 3GPP™ Std. TS 38.211 V17.5.0, Jun. 2023, Release 17.

[22] G. Torsoli, M. Z. Win, and A. Conti, "Selection of reference base station for TDOA-based localization in 5G and beyond IIoT," in *Proc. IEEE Global Telecomm. Conf.*, Rio de Janeiro, Brazil, Dec. 2022, pp. 317–322.

[23] *Technical Specification Group Radio Access Network; NR; Physical layer measurements*, 3GPP™ Std. TS 38.215 V17.2.0, Sept. 2022, Release 17.

[24] A. Conti, G. Torsoli, C. A. Gómez-Vega, A. Vaccari, G. Mazzini, and M. Z. Win, "3GPP-compliant dataset for xG location-aware networks," *IEEE Open J. Veh. Tech.*, 2024.

[25] J. Klemelä, *Smoothing of Multivariate Data: Density Estimation and Visualization*. John Wiley & Sons, 2009.

[26] C. M. Bishop, *Pattern Recognition and Machine Learning*. New York, NY, USA: Springer, 2006.

[27] *Technical Specification Group Radio Access Network; Study on channel model for frequencies from 0.5 to 100 GHz*, 3GPP™ Std. TR 38.901 V17.0.0, Mar. 2022, Release 17.

[28] *Technical Specification Group Radio Access Network; Study on NR Positioning Enhancements*, 3GPP™ Std. TR 38.857 V17.0.0, Mar. 2021, Release 17.

[29] S. Jaeckel, L. Raschkowski, K. Börner, and L. Thiele, "QuaDRiGa: A 3-D multi-cell channel model with time evolution for enabling virtual field trials," *IEEE Trans. Antennas Propag.*, vol. 62, no. 6, pp. 3242–3256, 2014.